Hurricane annual cycle controlled by both seeds and genesis probability

Wenchang Yang (杨文昌)[a,1], Tsung-Lin Hsieh[b], and Gabriel A. Vecchi[a,b]

[a]Department of Geosciences, Princeton University, Princeton, NJ 08544; and [b]High Meadows Environmental Institute, Princeton University, Princeton, NJ 08544

Edited by Michael E. Mann, The Pennsylvania State University, University Park, PA, and approved September 2, 2021 (received for review May 4, 2021)

Understanding tropical cyclone (TC) climatology is a problem of profound societal significance and deep scientific interest. The annual cycle is the biggest radiatively forced signal in TC variability, presenting a key test of our understanding and modeling of TC activity. TCs over the North Atlantic (NA) basin, which are usually called hurricanes, have a sharp peak in the annual cycle, with more than half concentrated in only 3 mo (August to October), yet existing theories of TC genesis often predict a much smoother cycle. Here we apply a framework originally developed to study TC response to climate change in which TC genesis is determined by both the number of pre-TC synoptic disturbances (TC "seeds") and the probability of TC genesis from the seeds. The combination of seeds and probability predicts a more consistent hurricane annual cycle, reproducing the compact season, as well as the abrupt increase from July to August in the NA across observations and climate models. The seeds-probability TC genesis framework also successfully captures TC annual cycles in different basins. The concise representation of the climate sensitivity of TCs from the annual cycle to climate change indicates that the framework captures the essential elements of the TC climate connection.

hurricane | tropical cyclone | annual cycle | TC seeds

Tropical cyclones (TCs) are a major natural hazard to life and property (1). Therefore, understanding TC frequency variability and change in response to climate forcing (2–4) is not only of fundamental scientific interest but also crucial in practice. Yet, understanding the connection between climate and TC frequency remains challenging (5–8). In fact, we still do not have a satisfying theory even for its annual cycle. A particularly interesting region is the North Atlantic (NA) basin, where TCs are usually called hurricanes (NA TCs and hurricanes are treated as interchangeable hereafter unless otherwise stated). While the large-scale environment in which TCs are embedded evolves smoothly from month to month, hurricane activity usually covers only a few months, with the most active 3 mo from August to October (Aug–Oct). In contrast, hurricane activity is much weaker in the other months, even in the early or middle summer when the thermal condition appears to favor hurricane development.

Fig. 1*A* shows the annual cycles of NA TC monthly frequency averaged over the recent decades (1980 to 2018) from both observations and climate model (Geophysical Fluid Dynamics Laboratory [GFDL]/High-Resolution Atmospheric Model [HiRAM]) historical simulations. The standout of months Aug–Oct is apparent for both observations and simulations. One simple way of measuring the sharpness of the annual cycle is the ratio of Aug–Oct accumulative value to that from all the other months. This sharpness index is almost 3 in observations (Fig. 1*B*), which means approximately three-quarters of TCs occur in Aug–Oct. It is slightly lower from the HiRAM simulations but is still more than double, equivalent to two-thirds of total TCs being in Aug–Oct. Another pronounced feature related to the sharp annual cycle is the abrupt increase of TC frequency from July to August, by more than 100% in HiRAM and almost 200% in observations (Fig. 1*C*). Besides observations and simulations from HiRAM, two other GFDL climate models also show qualitatively similar behavior (see *SI Appendix*, Fig. S1 for Atmospheric Model version 2.5 [AM2.5] and *SI Appendix*, Fig. S2 for Atmospheric Model version 2.5 using C360 grid [AM2.5C360]). In fact, the sharpness of hurricane season has already been noticed in literature as early as in the 1990s (9), and it has also been found that the annual cycle of more intense hurricanes is sharper than that of weaker tropical cyclones (9).

So what determines this peaked shape of annual cycle? One way to understand the control of TC frequency is to relate it to the sea surface temperature (SST) over the NA basin or its value relative to the tropical (30°S to 30°N) mean SST (5). However, the annual cycles of both SST and relative SST over the NA are smooth and approximately sinusoidal, yielding less sharp peaks over Aug–Oct (*SI Appendix*, Fig. S3). More sophisticated TC frequency theories usually link TC genesis to various forms of TC genesis indexes, which estimate the total impact of multiple crucial variables from the large-scale background environment. One particularly interesting index is the genesis probability, or probability of TC genesis from pre-TC tropical disturbances or seeds (3, 10, 11), which is closely linked to the dynamically derived ventilation index (VI) (10). Ventilation process is hostile to TC development, and a larger VI value tends to yield a lower genesis probability.

Lines in Fig. 1*A* show the annual cycles of genesis probability monthly climatology calculated from both "observations" (European Center for Medium-Range Weather Forecasts Reanalysis version 5 [ERA5]) and the HiRAM simulations. While the probability does have higher values in TC season in general, the peak of its annual cycle is, however, not as sharp as

Significance

Atlantic hurricanes have a sharp annual cycle with more than half count concentrated in only 3 mo of August to October, which is, however, usually not captured by traditional tropical cyclone (TC) genesis theory. We find that this issue can be addressed if we take into account variation of pre-TC vortex seeds and incorporate it into a two-stage TC development: emerging of pre-TC seeds and development of TCs from seeds, with the latter described by TC genesis probability. The two processes working together lead to the sharp annual cycle of Atlantic hurricanes. We also demonstrate that TC annual cycles from various ocean basins can be unified and understood in the new framework.

Author contributions: W.Y., T.-L.H., and G.A.V. designed research; W.Y. performed research; W.Y. analyzed data; W.Y. wrote the paper; and W.Y., T.-L.H., and G.A.V. interpreted results and refinement of the manuscript.

The authors declare no competing interest.

This article is a PNAS Direct Submission.

[1]To whom correspondence may be addressed. Email: wenchang@princeton.edu.

This article contains supporting information online at https://www.pnas.org/lookup/suppl/doi:10.1073/pnas.2108397118/-/DCSupplemental.

Published October 5, 2021.

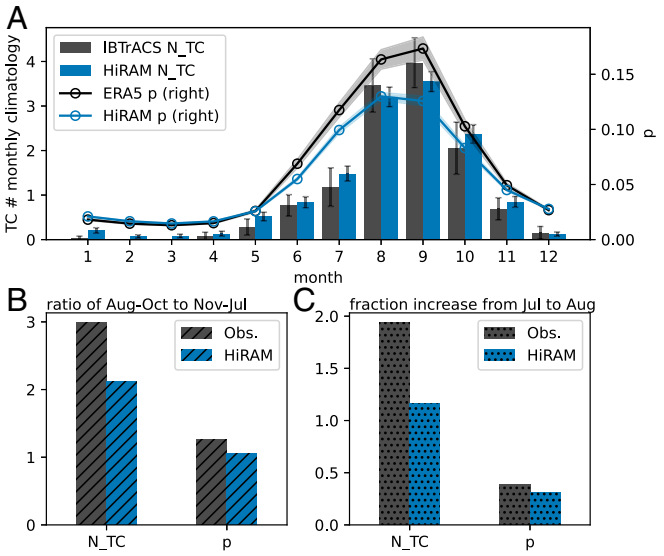

Fig. 1. Annual cycles of NA TC frequency and genesis probability and the sharpness indexes. (*A*) Monthly climatology of NA TC frequency (bars) and genesis probability index (lines) over the years of 1980 to 2018 from observations and HiRAM simulations. Observed TC frequency is from IBTrACS and genesis probability index is estimated using the ERA5 reanalysis monthly data. Error bars and shading areas indicate 95% confidence interval of the mean (multiyear mean for the observed and multiyear-and-ensemble mean for HiRAM simulation). (*B*) Ratio of accumulated value from Aug–Oct to that from Nov–Jul for TC frequency and genesis probability annual cycles in *A*. (*C*) Fraction increases of TC frequency and genesis probability from July to August in *A*.

the TC cycle. The sharpness index has a much lower value: close to one for both observations and simulations (Fig. 1*B*), which predicts a much lower fraction (around half) of the total TCs occur in Aug–Oct than the actual value. Neither does the genesis probability predict the abrupt increase of TCs from July to August (Fig. 1*C*). In fact, this is a generic problem also shared by many other forms of TC genesis indexes (12–16). While improvement can be made by incorporating more predictors from the large-scale environment into the indexes (17, 18), it is often achieved through complex statistical model fitting and therefore the physical process behind the improvement is unclear.

What causes the discrepancy between the NA TC annual cycle and that predicted by the genesis probability theory? One assumption from the probability theory is the constant supply of TC seeds. In other words, the frequency of tropical disturbances that have the potential to develop into TCs (depending on the genesis probability) does not change with time. Mathematically, the number of TCs is proportional to the number of seeds multiplied by the genesis probability:

$$N_{TC} \propto N_{seed} \times p(\Lambda). \quad [1]$$

The probability theory neglects the variation of N_{seed} and attributes TC variability solely to probability change. However, recent studies suggest that seeds play a crucial role in the response of TC genesis to climate change (3, 11, 19, 20). These studies demonstrated that the probability change alone is not able to explain the diverging responses of TC frequencies to radiative climate forcings from different climate models and numerical experiments, but the result is promising when taking into account the change of seeds. The question is whether the framework of probability and seeds combined together can help us better understand the hurricane annual cycle, which, like climate change, is also primarily driven by radiative forcing. While the signal of climate change often involves a large degree of uncertainty, the annual cycle of hurricanes is clearly defined in observations and well simulated in state-of-the-art high-resolution climate models, which is ideal to test the framework of probability and seeds.

Fig. 2 shows the annual cycles of TCs, probability, seeds, and the product of seeds and probability from observations as well as the three GFDL high-resolution climate models. To focus on the annual cycle, all the quantities are normalized by their annual total value. For observations (Fig. 2*A*), the NA TC annual cycle predicted by the product of seeds and probability is greatly sharpened compared to that predicted by probability alone. As a result, the predicted annual cycle by the seeds-probability framework is much more consistent with the target TC annual cycle. The improvement of the annual cycle prediction can be attributed to the also relatively high value of seed number during the TC season, although the seed annual cycle is much more flat. The predicted TC annual cycles by the seeds-probability framework are also sharper and more correlated to the actual cycles from the three climate model simulations (Fig. 2 *B–D*). As a result, the sharpness index of $N_{seed} \times p$ largely increases from probability alone and is more consistent with that of TCs (*SI Appendix*, Fig. S4). Additionally, the abrupt change of TC frequency from July to August is also well captured in the seeds-probability framework (*SI Appendix*, Fig. S5). Note that while climate model simulations generally capture the observed TC annual cycle, the October normalized TC number is higher than that observed, especially for AM2.5 and AM2.5C360. This appears to be linked to the biased seed number from simulations, with their genesis location mainly over the eastern NA basin off the coast of West Africa in HiRAM (*SI Appendix*, Figs. S6 and S7) but the western NA basin in AM2.5 and AM2.5C360 (*SI Appendix*, Figs. S8 and S9). What causes this October seed bias needs further examination.

An alternative way to demonstrate the superiority of the probability and seeds framework is to compare the scatter plot of TCs versus probability to that of TCs versus the product of probability and seeds (Fig. 3) (all quantities are normalized by the annual total value). Note that data from both observations and all the three model simulations are now put together in the same scatter plot. While the probability can explain the TC annual cycle to some extent, the framework of probability and seeds has at least three advantages: 1) $N_{seed} \times p$ can explain a larger fraction of variance from TCs (0.97 vs. 0.83), 2) the coefficient of normalized TCs regressed on the predictor is close to one, and 3) the intercept of the regression is close to zero.

The framework of probability and seeds still holds if we add monthly climatology values from the six other major TC basins besides the NA, including the eastern Pacific (EA), western North Pacific (WP), northern Indian Ocean (NI), southern Indian Ocean (SI), Australia (AU), and southern Pacific (SP) basins as shown in Fig. 4. Now we look at the scatter plots from observations and the three models separately but include data from different basins. By comparison, the NA TC has the largest single-month normalized TC frequency (in September), which makes its annual cycle the sharpest. Overall, the framework of probability and seeds works much better than the probability framework in both observations and the three climate models.

Summary and Discussion

In this study, we attempt to address the fundamental issue of TC annual cycle, which provides an observationally constrained test on theories of TC climatology. Current genesis probability theory usually predicts a much smoother annual cycle and is difficult to capture the sharpness of the TC season. By taking into account seed variability, we demonstrate that the seeds-probability framework reproduces the hurricane annual cycle much more consistently than the probability alone and, in particular, is able

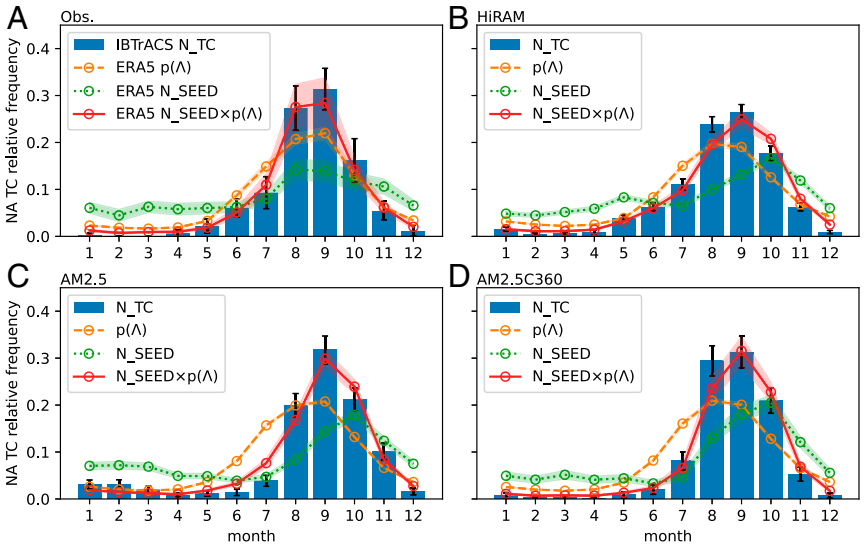

Fig. 2. Monthly climatologies of NA TC relative frequency (normalized by the total number of the 12 mo, blue bars) and those predicted by TC genesis probability (orange dashed line), frequency of vortex seeds (green dotted line), and combination of both (red solid line). (*A*) Observations (Obs.), (*B*) model historical simulations from HiRAM, (*C*) AM2.5, and (*D*) AM2.5C360. Error bars and shading areas show the 95% confidence interval of the mean.

to capture the sharp hurricane season. It also provides a unified framework to view TC annual cycles from various basins, sources (both observations and climate models), and numerical experiments.

Previous studies have shown that the probability and seeds framework could help explain diverging responses of TC frequency to radiative climate forcing induced by greenhouse gases (3, 11, 21, 22). Here we test and validate that the seeds-probability framework also works in a different scenario: climatological variations driven by the annual cycle radiative forcing. This study applies the framework to explain the TC annual cycle. The two-step thinking of TC genesis (i.e., seed genesis and then TC genesis) might help explain the early finding that more intense hurricanes have a much sharper annual cycle than do weaker TCs. Assume that disturbances at the very initial stage have a relatively flat annual cycle and eventually develop into intense hurricanes after multiple steps, of which each step is governed by a probability with an annual cycle shape peaking more or less around the TC season. Then the initial relatively flat annual cycle of disturbances would ultimately become much sharper after being multiplied by a chain of such probabilities (see *SI Appendix*, Fig. S10, which provides a preliminary support to this hypothesis). This is more likely the case for the stage from a TC seed to an intense hurricane since the probability of each step over this stage might share a similar relationship with the large-scale environment. Probabilities in the early stage from the initial disturbance to a seed appear to be governed by different mechanisms (11).

As the probability and seeds framework seems to work across a broad range of different climate-forcing scenarios, the immediate question arises: Does it also work in the case of unforced or internal variability-dominated climate variation? For example, can we use this framework to understand different TC frequencies in El Niño versus La Niña years, as well as contributions from seeds and probability in extreme TC years? Another question, which is more fundamental, is, What controls the variability of seeds? Can we model the seed frequency variability in a similar way to the TC frequency? While wind shear dominates the NA TC genesis probability annual cycle (*SI Appendix*, Fig. S11), our preliminary analysis suggests that vertical velocity variability plays a dominant role in the seed genesis index proposed by Hsieh et al. (11) (*SI Appendix*, Fig. S12). This may explain why statistical models of TC genesis can be improved by incorporating vertical velocity (18) or instability (17). More comprehensive analysis and examination are needed to address all these important questions.

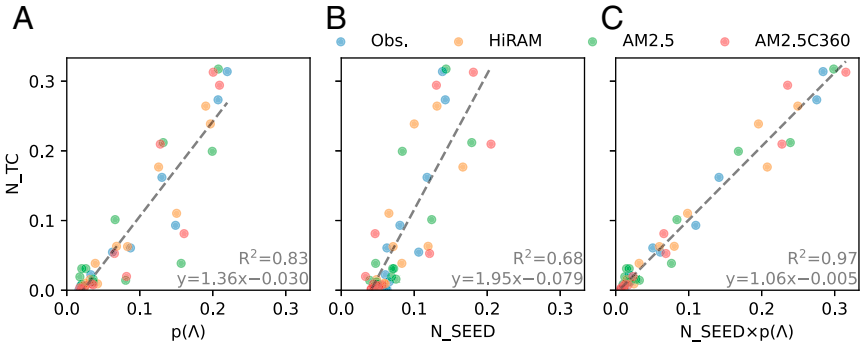

Fig. 3. Scatter plots of monthly climatology of NA TC frequency versus TC genesis probability index (*A*), frequency of vortex seeds (*B*), and the combination of both (*C*) from observations and model historical simulations from HiRAM, AM2.5, and AM2.5C360. All the quantities are normalized by their annual total. Dashed lines show the linear regression, for which the equation and the variance explained are shown on the bottom right of each panel.

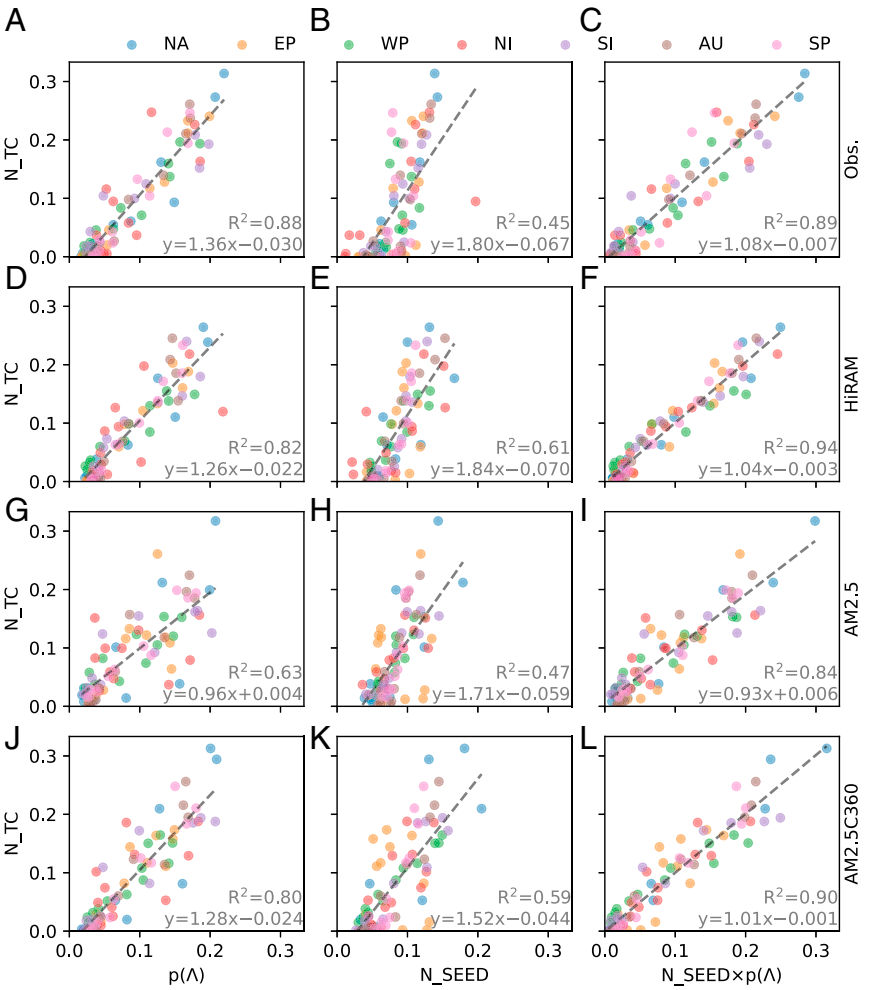

Fig. 4. Scatter plots of monthly climatologies of TC frequency versus TC genesis probability index (*A*, *D*, *G*, *and J*), frequency of vortex seeds (*B*, *E*, *H*, *and K*), and the product of both (*C*, *F*, *I*, and *L*) over the seven major TC basins of NA, EP, WP, NI, SI, AU, and SP from observations (*A*–*C*) and model historical simulations from HiRAM (*D*–*F*), AM2.5 (*G*–*I*), and AM2.5C360 (*J*–*L*). Dashed lines show the linear regression, for which the equation and the variance explained are shown on the bottom right of each panel.

Materials and Methods

Data. For observed TC tracks, we use version 4 of International Best Track Archive for Climate Stewardship (IBTrACS v04) (23). The ERA5 reanalysis dataset (24) is used to track seeds of TCs, where instantaneous hourly data at Coordinated Universal Time hours of 00, 06, 12, and 18 (four times daily) are used. We also use ERA5 reanalysis monthly data to calculate large-scale climate environment variables and the associated TC genesis probability.

Model and Numerical Experiments. In this study, we use three Atmospheric General Circulation Models from GFDL that share the same dynamical core but vary in atmospheric physics or horizontal resolution, including HiRAM (25), AM2.5, and AM2.5C360. HiRAM has a horizontal resolution of about 50 km and is able to simulate many aspects of the observed TC frequency variability over the past few decades during which reliable observations are available. AM2.5 has the same horizontal resolution of 50 km as HiRAM but uses the relaxed Arakawa–Schubert convective closure instead of the scheme based on the parameterization of shallow convection from the University of Washington (26) used in HiRAM. AM2.5C360 is the same as AM2.5 except the horizontal resolution is doubled to about 25 km. Using HiRAM, AM2.5, and AM2.5C360, we performed Atmospheric Model Intercomparison Project (AMIP)-type ensemble simulations (five ensemble members from HiRAM and AM2.5 and three ensemble members from AM2.5C360) in which the atmospheric model is forced by SST from Hadley Centre Sea Ice and Sea Surface Temperature dataset version 1 (27) over the period of 1971 to 2018. All the ensemble members are forced by the same historical SST and differ only in initial condition. For both observational data and model output from the AMIP historical runs, only years of 1980 to 2018 are focused on and analyzed unless otherwise stated.

TC and Seed Tracking. To track TCs, we use the TC tracking algorithm developed by Harris et al. (28) and briefly describe it here as follows: The input data for the tracking algorithm include 6-hourly instantaneous sea level pressure (SLP), 850 hPa vorticity, 10-m wind speed, and middle-troposphere (300 to 500 hPa) air temperature. The whole process can be decomposed into two steps. In step 1, storms are first tracked based on SLP, where a maximum 850-hPa cyclonic vorticity magnitude of at least 1.5×10^{-4} s^{-1} is applied to filter out weak or disorganized systems. In step 2, three lifetime-related conditions are applied on each storm track to get only long-lived TCs. The three minimum lifetimes are 1) 72 h of total lifetime, 2) 48 h of cumulative warm core condition, and 3) 36 consecutive hours of both warm core and maximum 10-m wind speed greater than tropical-storm strength (17.5 $m \cdot s^{-1}$). The warm core condition here means the maximum middle-troposphere (300 to 500 hPa) temperature is encircled by a 2 °C (critical temperature difference) contour and is no more than 500 km (offset radius) from the storm center of SLP.

In our application to the HiRAM TC tracking, we reduce the maximum 10-m wind speed threshold from 17.5 to 15.75 $m \cdot s^{-1}$ in the 36 consecutive hours condition but do require the maximum of 10-m maximum wind speed along each storm track is at least 17 $m \cdot s^{-1}$. We also modify the warm core condition by increasing the critical temperature difference from 2 to 2.5 °C and reducing the offset radius from 500 to 110 km. AM2.5 and AM2.5C360 apply the same protocol, except using a critical temperature difference of 1 °C and the default 2 °C, respectively.

To track vortex seeds, we use the rain cluster tracking algorithm developed by Hsieh et al. (11), which tracks contiguous grid cells whose precipitation rates are larger than the 99.5th percentile of all the tropical (30°S to 30°N) grids at each time step. Clusters are required to be larger than four grid points, last longer than 1 d, and initiate within 30°S to 30°N. Seeds are defined as the tracks of the rain cluster whose maximum 850-hPa vorticity along the track exceeds 4×10^{-4} s^{-1} and duration over the ocean surface is at least 12 h. Our results are generally robust to choice of vorticity or ocean hour thresholds (*SI Appendix*, Figs. S13–S15). We have also tested an alternative seed definition based on SLP that starts from step 1 of TC tracking described above and further require that the tracks start within 30°S to 30°N and last at least 12 h over the ocean surface. The annual cycles predicted using this alternative definition are similar to those using rain cluster (*SI Appendix*, Fig. S16).

Ventilation Index and TC Genesis Probability. Ventilation index is calculated using equation 1 of ref. 10:

$$\Lambda = \frac{u_{shear}\chi_m}{u_{PI}}, \quad [2]$$

where u_{shear} is the vertical wind shear between 850 and 200 hPa, χ_m is the entropy deficit, and u_{PI} is the potential intensity. Based on the logistic regression model (logistic relationship between probability and the logarithm of ventilation index), TC genesis probability is linked to the ventilation index through

$$p(\Lambda) = \frac{1}{1 + (\Lambda/\Lambda_0)^n}, \quad [3]$$

where the parameters of Λ_0 and n are selected to be in agreement with Tang and Emanuel (10) so that $p(0.014) = 0.5$ and $p(0.1) = 0.1$. As a result, we get $\Lambda_0 = 0.014$ and $n = \log(9)/\log(0.1/0.014) \approx 1.1$.

We first calculate monthly TC genesis probability at each longitude/latitude grid point and then perform spatial average weighted by grid area between 10°N (S) and 30°N (S) for the Northern (Southern) Hemisphere basins. We have also tested the sensitivity to the alternative choice in which genesis probability is averaged between 5°N (S) and 30°N (S) and the result is similar (*SI Appendix*, Fig. S17). These multiyear (and multiensemble for model simulations) basin-mean monthly TC genesis probability time series are thereafter used for the estimation of annual cycles for each basin.

TC Basins. Seven global TC basins covered in this study are defined the same as that in figure S4 of Yang et al. (4), including the NA, EP, WP, NI, SI, AU, and SP basins.

Normalized Annual Cycle. For TC frequency, genesis probability, and seed frequency, the order of processing data is 1) calculation of monthly time series for each basin, 2) calculation of monthly climatologies, and 3) normalization of monthly climatologies by the annual total. For the predictor of $N_{seed} \times p$, the multiplication takes place between the first and second steps in the above process.

Data Availability. The IBTrACS v04 dataset is available from National Oceanic and Atmospheric Administration (NOAA), https://www.ncdc.noaa.gov/ibtracs. The ERA5 dataset is available from European Centre for Medium-Range Weather Forecasts (ECMWF), https://www.ecmwf.int/en/forecasts/datasets/reanalysis-datasets/era5. Codes and all other data for the results of this study are available from GitHub, https://github.com/wy2136/tc_annual_cycle.

ACKNOWLEDGMENTS. The simulations presented in this article were performed on computational resources managed and supported by Princeton Research Computing, a consortium of groups including the Princeton Institute for Computational Science and Engineering and the Office of Information Technology's High Performance Computing Center and Visualization Laboratory at Princeton University. This work is supported by NOAA/Ocean Climate Observation Program (OCO) (Award NA18OAR4310418), NOAA/Modeling, Analysis, Predictions, and Projections (MAPP) (Award NA18OAR4310273), and the Carbon Mitigation Initiative at Princeton University.

1. K. Emanuel, Tropical cyclones. *Annu. Rev. Earth Planet. Sci.* **31**, 75–104 (2003).
2. F. S. R. Pausata, S. J. Camargo, Tropical cyclone activity affected by volcanically induced ITCZ shifts. *Proc. Natl. Acad. Sci. U.S.A.* **116**, 7732–7737 (2019).
3. G. A. Vecchi *et al*., Tropical cyclone sensitivities to CO_2 doubling: Roles of atmospheric resolution, synoptic variability and background climate changes. *Clim. Dyn.* **53**, 5999–6033 (2019).
4. W. Yang *et al*., Climate impacts from large volcanic eruptions in a high-resolution climate model: The importance of forcing structure. *Geophys. Res. Lett.* **46**, 7690–7699 (2019).
5. T. R. Knutson *et al*., Tropical cyclones and climate change. *Nat. Geosci.* **3**, 157–163 (2010).
6. K. J. Walsh *et al*., Tropical cyclones and climate change: Tropical cyclones and climate change. *Wiley Interdiscip. Rev. Clim. Change* **7**, 65–89 (2016).
7. T. Knutson *et al*., Tropical cyclones and climate change assessment: Part I: Detection and attribution. *Bull. Am. Meteorol. Soc.* **100**, 1987–2007 (2019).
8. T. Knutson *et al*., Tropical cyclones and climate change assessment: Part II: Projected response to anthropogenic warming. *Bull. Am. Meteorol. Soc.* **101**, E303–E322 (2020).
9. C. W. Landsea, A climatology of intense (or major) Atlantic hurricanes. *Mon. Weather Rev.* **121**, 1703–1713 (1993).
10. B. Tang, K. Emanuel, A ventilation index for tropical cyclones. *Bull. Am. Meteorol. Soc.* **93**, 1901–1912 (2012).
11. T. L. Hsieh, G. A. Vecchi, W. Yang, I. M. Held, S. T. Garner, Large-scale control on the frequency of tropical cyclones and seeds: A consistent relationship across a hierarchy of global atmospheric models. *Clim. Dyn.* **55**, 3177–3196 (2020).
12. S. Camargo, A. H. Sobel, A. G. Barnston, K. A. Emanuel, Tropical cyclone genesis potential index in climate models. *Tellus A* **59**, 428–443 (2007).
13. S. J. Camargo, K. A. Emanuel, A. H. Sobel, Use of a genesis potential index to diagnose ENSO effects on tropical cyclone genesis. *J. Clim.* **20**, 4819–4834 (2007).
14. M. K. Tippett, S. J. Camargo, A. H. Sobel, A Poisson regression index for tropical cyclone genesis and the role of large-scale vorticity in genesis. *J. Clim.* **24**, 2335–2357 (2011).
15. C. L. Bruyère, G. J. Holland, E. Towler, Investigating the use of a genesis potential index for tropical cyclones in the North Atlantic basin. *J. Clim.* **25**, 8611–8626 (2012).
16. C. E. Menkes *et al*., Comparison of tropical cyclogenesis indices on seasonal to interannual timescales. *Clim. Dyn.* **38**, 301–321 (2012).
17. M. DeMaria, J. A. Knaff, B. H. Connell, A tropical cyclone genesis parameter for the tropical Atlantic. *Weather Forecast.* **16**, 219–233 (2001).
18. B. Wang, H. Murakami, Dynamic genesis potential index for diagnosing present-day and future global tropical cyclone genesis. *Environ. Res. Lett.* **15**, 114008 (2020).
19. S. Yokoi, Y. N. Takayabu, Multi-model projection of global warming impact on tropical cyclone genesis frequency over the western North Pacific. *J. Meteorol. Soc. Jpn.* **87**, 525–538 (2009).
20. T. Li *et al*., Global warming shifts Pacific tropical cyclone location. *Geophys. Res. Lett.* **37**, L21804 (2010).
21. M. Sugi *et al*., Future changes in the global frequency of tropical cyclone seeds. *Sci. Online Lett. Atmos.* **16**, 70–74 (2020).
22. Y. Yamada *et al*., Evaluation of the contribution of tropical cyclone seeds to changes in tropical cyclone frequency due to global warming in high-resolution multi-model ensemble simulations. *Prog. Earth Planet. Sci.* **8**, 11 (2021).
23. K. R. Knapp, M. C. Kruk, D. H. Levinson, H. J. Diamond, C. J. Neumann, The International Best Track Archive for Climate Stewardship (IBTrACS): Unifying tropical cyclone data. *Bull. Am. Meteorol. Soc.* **91**, 363–376 (2010).
24. H. Hersbach *et al*., The ERA5 global reanalysis. *Q. J. R. Meteorol. Soc.* **146**, 1999–2049 (2020).
25. M. Zhao, I. M. Held, S. J. Lin, G. A. Vecchi, Simulations of global hurricane climatology, interannual variability, and response to global warming using a 50-km resolution GCM. *J. Clim.* **22**, 6653–6678 (2009).
26. C. S. Bretherton, J. R. McCaa, H. Grenier, A new parameterization for shallow cumulus convection and its application to subtropical cloud-topped boundary layers. Part I: Description and 1d results. *Mon. Weather Rev.* **132**, 864–882 (2004).
27. N. A. Rayner *et al*., Global analyses of sea surface temperature, sea ice, and night marine air temperature since the late nineteenth century. *J. Geophys. Res.* **108**, 4407 (2003).
28. L. M. Harris, S. J. Lin, C. Tu, High-resolution climate simulations using GFDL HiRAM with a stretched global grid. *J. Clim.* **29**, 4293–4314 (2016).